Journal of Applied Polymer Science

In situ polymerization of bio-based thermosetting polyurethane/graphene oxide nanocomposites

Jing Zhang,[1,2] Chaoqun Zhang,[1] Samy A. Madbouly[1,3]

[1]Department of Materials Science and Engineering, Iowa State University, Ames, Iowa

[2]Department of Corrosion Prevention and Polymer Materials, College of Materials Science and Engineering, Jiangsu University of Science and Technology, Zhenjiang, China

[3]Department of Chemistry, Faculty of Science, Cairo University, Orman-Giza 12613, Egypt

Correspondence to: S. A. Madbouly (E-mail: madbouly@iastate.edu)

ABSTRACT: Novel bio-based polyurethane/graphene oxide (GO) nanocomposites have been successfully synthesized from biorenewable epoxidized soybean-castor oil fatty acid-based polyols with considerable improvement in mechanical and thermal properties. The GO was synthesized via a modified pressurized oxidation method, and was investigated using Raman spectra, AFM and XPS, respectively. The toughening mechanism of GO in the bio-based polyurethane matrix was explored. The elongation at break and toughness of polyurethane were increased by 1.3 and 0.8 times with incorporation of 0.4 wt % GO, respectively. However, insignificant changes in both mechanical strength and modulus were observed by adding GO. The results from thermal analysis indicated that the GO acts as new secondary soft segments in the polyurethane which lead to a considerable decrease in the glass transition temperature and cross-link density. The SEM morphology of the fracture surface after tensile testing showed a considerable aggregation of graphene oxide at concentrations above 0.4 wt %. © 2014 Wiley Periodicals, Inc. J. Appl. Polym. Sci. **2015**, *132*, 41751.

KEYWORDS: biopolymers & renewable polymers; composites; graphene and fullerenes; mechanical properties; nanotubes; thermal properties

Received 19 August 2014; accepted 11 November 2014

DOI: 10.1002/app.41751

INTRODUCTION

The high cost of petroleum-based products, their negative impact on the environment, and the scarcity of nonrenewable resources are the main factors encouraging us to synthesis and develop a new class of environmentally friendly, nanostructured bio-based polymer composites with prescribed macromolecular structure, mechanical and thermal property. Polyurethanes (PU) are most versatile synthetic polymer materials that have been used with diverse industrial applications for many decades. PU can be tailored to meet the highly diversified demands of modern technologies.[1] The PU are segmented polymers comprising of alternating sequences of soft and hard segments with unique microphase-separated structure and prescribed mechanical and thermal properties.[2,3] Extensive studied have done in literature to understand the relationship between chemical structure and properties of various kinds of polyurethanes.[4–6] By varying the structure, molecular weight of the segments, and the ratio of the soft to the hard segments, a broad range of physical properties can be obtained. The materials can be hard and brittle, soft and tacky, or anywhere in between. In industry, only a few polyisocyanates are commonly used, while a variety of polyols are available. Therefore, the choice of polyol typically determines the properties of the created polyurethane. In addition to petroleum-based polyols, vegetable oils, such as soybean oil,[7] canola oil,[8,9] palm oil,[10,11] sunflower oil, corn oil, and linseed oil,[12–14] have been extensively studied as bases for various polyols used for the manufacture of PUs with high thermal stability and mechanical properties. As already mentioned above, the increasing environmental burden and price of crude oil have triggered great interest in the development of bio-base polyols. Vegetable oils are inexpensive sustainable materials that can be used to synthesize a wide range of polyols with different numbers of hydroxyl groups. The reason of selecting castor oil in the current study based on the fact that about 90% of the fatty acid chains in the castor oil bearing a hydroxyl group, eliminates the need for chemical modification of the triglyceride to produce polyols for PU synthesis.

Graphene oxide (GO) can be made from chemical exfoliation by reactions that have been known for 150 years. Recently,

Additional Supporting Information may be found in the online version of this article.

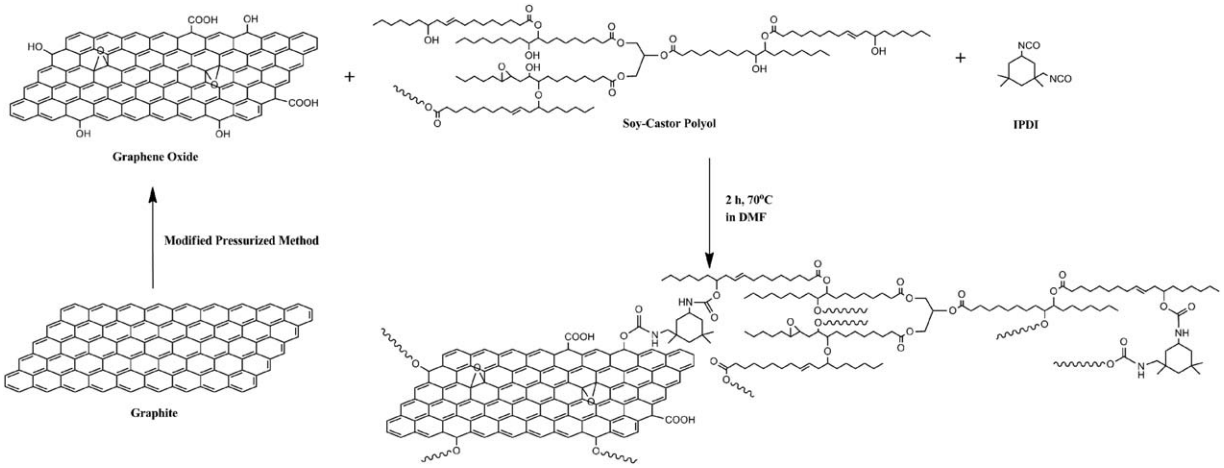

Figure 1. Elementary steps for the synthesis of PU/GO nanocomposite.

interest in this old material has resurged, because GO is a promising solution-processable precursor for the bulk production of graphene. There are abundant oxygenated functional groups on GO's basal plane and edges, such as carboxyl, hydroxyl, and epoxy. Moreover, GO is a two-dimensional sheet with feature sizes at two abruptly different length scales. The apparent thickness of GO is approximately 1 nm, while the lateral dimensions can range from several nanometers to hundreds of micrometers. The disocynate can react easily with the oxygenated functional groups attached to GO to produce exfoliated PU nanocomposites with enhanced mechanical, physical and thermal properties. Nguyen *et al.* prepared a cast nanocomposite film from a mixture of thermoplastic polyurethane (TPU) solution and functionalized graphene sheet (FGS) suspended in methyl ethyl ketone. The FGS efficiently reinforced the TPU matrix particularly in the temperature region above the soft segment melt.[15] Cai *et al.* reported the substantial improvement in the stiffness, toughness and thermal stability of linear PU resulting from the incorporation of GO.[16] Kim *et al.* reported exfoliated GO reinforced TPU nanocomposites with improved gas barrier and electrical conductivity.[17] Lee *et al.* prepared waterborne polyurethane (WPU) nanocomposites with functionalized graphene sheets by *in situ* method; the conductivity and modulus of nanocomposites improved, while the thermal stability and tensile strength of nanocomposites deteriorated.[18] Wang *et al.* prepared GO sheets reinforced linear PU composites by *in situ* polymerization. The authors found that, the nanocomposites displayed high electrical conductivity and good thermal stability.[19] Chen and Lu reported simultaneous improvement in strength and toughness while maintaining the good ductility of polyurethane elastomers by adding FGS.[20] Little work has been reported for bio-based PU nanocomposites.

The present article will consider in detail the effects of surface modified GO on the mechanical, thermal, and morphological properties of bio-based PU. The thermosetting PU will be synthesized from epoxidized soybean oil and castor oil fatty acid. Various analytical techniques, such as, Raman spectra, AFM, XPS, DSC, DMA, TGA, SEM, and mechanical test will be used to characterize the PU/GO nanocomposites and understand the structure–property relationship. The *in situ* polymerization of bio-based and surface modified GO could produce nanostructured composite with enhanced benefits.

EXPERIMENTAL

Materials

Castor oil, graphite flakes (100 mesh), isophorone diisocyanate (IPDI), and dibutyltin dilaurate (DBTDL) were purchased from Sigma-Aldrich Ltd. Epoxidized soybean oil with approximately 4.5 oxirane rings per triglyceride was purchased from Scientific Polymer Inc., New York, NY. Potassium permanganate ($KMnO_4$), Magnesium sulfate ($MgSO_4$), hydrochloric acid (HCl), sulfuric acid (H_2SO_4), hydrogen peroxide (H_2O_2, 30% aq.), methyl ethyl ketone (MEK), and *N*,*N*-dimethylformamide (DMF) were provided by Fisher Ltd.

Preparation of Bio-Based Polyols

The soy-castor oil based polyols were prepared via ring opening reaction between epoxidized soybean oil and castor oil fatty acid. The castor oil fatty acid and epoxidized soybean oil were mixed at 130 to 170°C in a flask with a magnetic stirrer and maintained in dry nitrogen atmosphere. After several hours, a polyol as a light reddish/yellow, viscous liquid was obtained. More details about the synthesis of polyol from castor oil fatty acid and epoxidized soybean oil can be found in our earlier work.[21]

Preparation of the Graphene Oxide

Graphene oxide was synthesized via a modified pressurized oxidation method. Graphite, $KMnO_4$, H_2SO_4 (98%), teflon reactor, and stainless steel autoclave were completely cooled respectively in a refrigerator at 0 to 4°C before use. Firstly, the cooled graphite (2 g) and $KMnO_4$ (10 g) were put into the reactor, and then, H_2SO_4 (100 mL) was added to the reagent mixture. As soon as the sulfuric acid was added, the reactor that filled with reagent mixture was moved into an ice water bath and kept mechanical stir at 800 rpm for 1 h. After that, the reactor filled with reagent mixture was put into the stainless steel autoclave and tightly covered. The autoclave was heated at 80°C in an oven for 2 h. The obtained mud was diluted with a large amount of deionized water. With mechanical stirring, H_2O_2

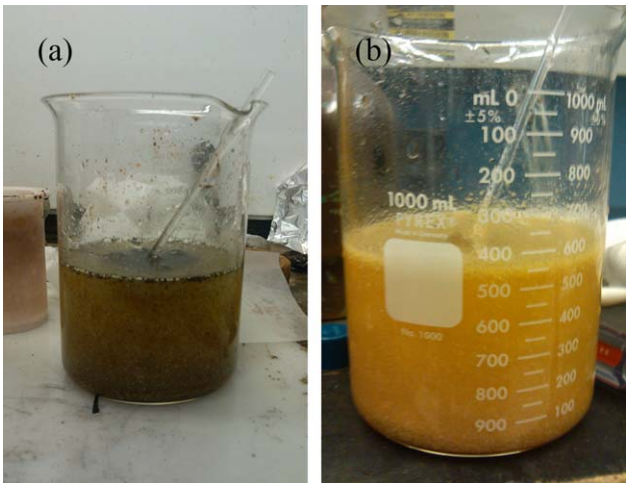

Figure 2. The GO sample after addition of H_2O_2: (a) pressurized oxidation method, and (b) modified pressurized oxidation method. [Color figure can be viewed in the online issue, which is available at wileyonlinelibrary.com.]

(30%) was dripped into the suspension until the slurry turned golden yellow. The suspension was washed with hot HCl and deionized water until the pH reached 7.0 to obtain the GO.

Preparation of the Bio-Based PU/GO Nanocomposites

The obtained GO was dried at 60°C under vacuum overnight. The dried GO (0.1 g) was exfoliated in 10 g DMF using ultrasonication with a power of 70 W for 0.5 h at room temperature. Calculated amount of the obtained GO/DMF mixture was mixed with 1 g bio-based polyols at room temperature, and then 0.31 g IPDI and one to two drops DBTDL catalyst were added to the mixture and kept stirring at 70°C for 2 h. Afterward, the solution was poured into a teflon mold to produce 100 mm length and 50 mm width film with approximately 0.5 mm thickness, which were cut into specific dimensions for characterization. The elementary steps of PU/GO synthesis is illustrated in Figure 1.

Characterization

Raman spectra were performed using a Renishaw inVia Raman Microscope with excitation by a 532 nm argon laser. Atomic force microscopy (AFM) observations of GO were obtained using a dimension 3000 scanning probe microscope (Bruker) under tapping mode. The GO was dispersed in deionized water for 0.5 h using 70 W ultrasonication. The obtained brown GO dispersion was diluted by deionized water into almost transparent dispersion, and then dip-coated onto freshly cleaved mica surface and dried at room temperature before observation. X-ray photoelectron spectroscopy (XPS) of dried GO was carried out using a physical electronics 5500 multitechnique system. The excitation source was a monochromatic Al-Kα radiation.

The mechanical properties of the PU and PU/GO nanocomposite films were determined using an Instron universal testing machine (model 4502) with a crosshead speed of 100 mm min^{-1}. Rectangular specimens of 50 mm × 10 mm (length × width) were used. Average values of at least five replicates of each sample were taken. The toughness of the materials was obtained from the area under the corresponding tensile stress–strain curves.

Dynamic mechanical analysis (DMA) of the neat PU and PU/GO nanocomposite films was performed using a TA instrument (DMA Q800 dynamic mechanical analyzer) with a film-tension mode of 1 Hz. Approximately 0.5 mm × 10 mm (thickness × width) rectangular specimens were used for the DMA measurements. The samples were cooled and held isothermally at −80°C for 3 min before the temperature increased to 120°C at a rate of 5°C min^{-1}. The glass transition temperatures (T_g) of the samples were obtained from the peaks of the tan δ curves. Differential scanning calorimetry (DSC) measurements for the materials were carried out using a TA instrument Q2000. The samples were heated from room temperature to 90°C at a heating rate of 20°C min^{-1} to erase their thermal history, equilibrated at −90°C and then heated to 90°C at a heating rate of 20°C min^{-1}. The T_g of the samples were determined from the midpoint temperature in the heat capacity change of the second DSC scan. Samples of 5 mg were cut from the films and used for the measurements. The thermogravimetric analysis (TGA) measurements were carried out using a Q50 thermogravimetric analyzer (TA Instruments, New Castle, DE). For the TGA measurement, about 5 mg of the nanocomposite was heated from 30 to 700°C under a nitrogen atmosphere at 20°C/min heating rate.

The fracture surfaces of samples were examined using post-tensile testing with a scanning electron microscopy (SEM, FEI Quanta 200) to evaluate the GO dispersion and correlate the fracture morphologies with mechanical properties.

RESULTS AND DISCUSSION

Preparation and Characterization of GO

It is well established that the most promising method for a large-scale production of GO, which is obviously important for the practical application of polymer/GO nanocomposites, is based on the oxidation and exfoliation of graphite. The Hummers and Staudenmaier methods are the most widely used

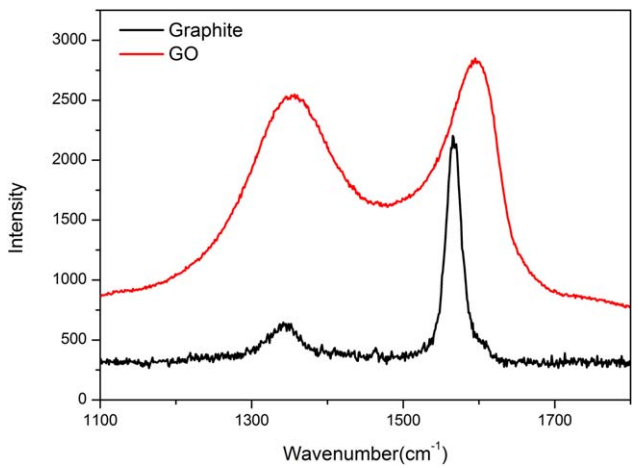

Figure 3. Raman spectra of graphite and GO obtained from the modified pressurized oxidation method. [Color figure can be viewed in the online issue, which is available at wileyonlinelibrary.com.]

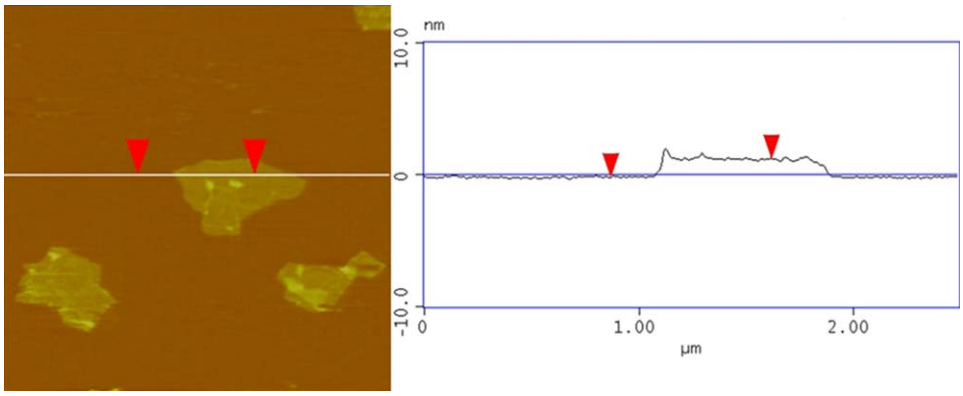

Figure 4. AFM profile for GO obtained from the modified pressurized oxidation method. [Color figure can be viewed in the online issue, which is available at wileyonlinelibrary.com.]

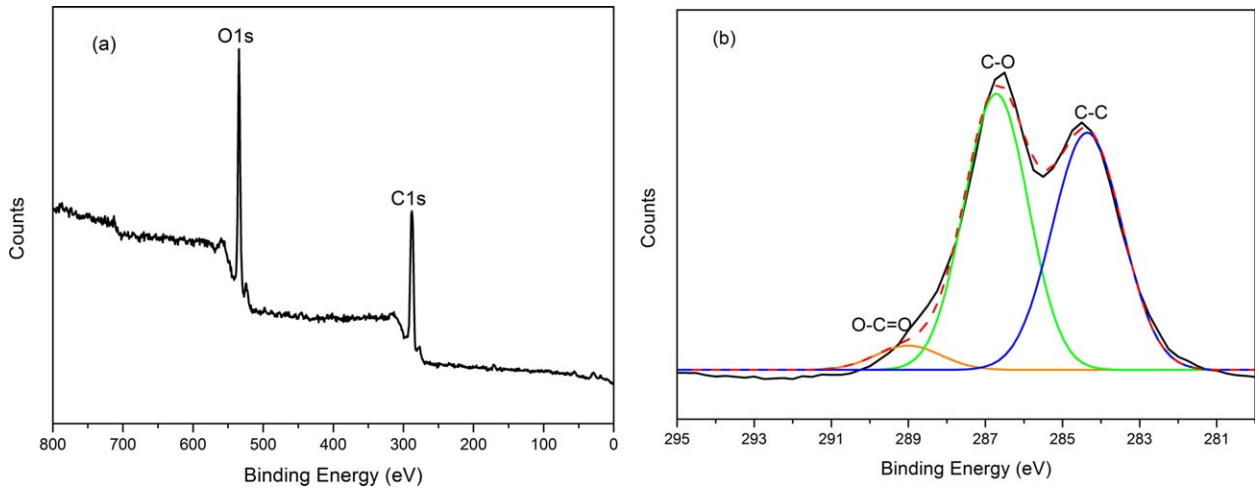

Figure 5. (a) XPS curve of GO, (b) XPS C1s core-level spectra of GO. [Color figure can be viewed in the online issue, which is available at wileyonlinelibrary.com.]

methods to prepare GO, using strong oxidants in the presence of strong acid.[22,23] Very careful temperature control and experimental operation are usually required. Moreover, it needs around 100 hours to complete the reaction. In order to solve these problems, Bao *et al.* developed a pressurized oxidation method based on the Hummers approach to prepare GO, which only needs much easier operations and less time.[24] Figure 2(a) showed the GO control sample obtained from the pressurized oxidation method after addition of H_2O_2. The control sample was partially turned into yellow and bearing a lot of black impurities which are graphite with incomplete oxidation or without oxidation. As for the pressurized oxidation method, the graphite and strong oxidants mixture were kept stand still under 0 to 4°C for 1.5 h to make the graphite to be invasive and intercalated by H_2SO_4. The pressurized oxidation method was modified by employing mechanical stir to the graphite and strong oxidants mixture to enhance the diffusion process. Figure 2(b) presents the GO obtained by modified pressurized

Table I. Tensile Mechanical Property of Neat PU and GO/PU Nanocomposites

	Tensile strength (MPa)	Young's modulus (MPa)	Elongation at break values (%)	Toughness (MPa)
Neat PU	8.8 ± 0.4	12.4 ± 0.5	114.8 ± 8.9	4.6
0.2% GO/PU	6.9 ± 0.3	4.8 ± 0.4	229.5 ± 18.2	8.4
0.4% GO/PU	6.6 ± 0.2	3.1 ± 0.4	266.8 ± 15.0	8.5
0.6% GO/PU	5.6 ± 0.2	2.8 ± 0.2	251.1 ± 16.6	7.2
0.8% GO/PU	4.3 ± 0.1	2.4 ± 0.2	199.4 ± 12.3	4.6

Table II. Thermal Properties of Neat PU and GO/PU Nanocomposites Based on DMA and DSC

	Storage modulus at −80°C (MPa)	Initial transition temperature (°C)	$T_{g(DMA)}$ (°C)	$T_{g(DSC)}$ (°C)
Neat PU	1335	6.1	35.9	4.8
0.2% GO/PU	1411	−12.2	34.0	4.63
0.4% GO/PU	1614	−12.3	32.9	−8.5
0.6% GO/PU	1513	−3.7	31.5	−8.4
0.8% GO/PU	1386	−11.3	31.6	−8.2

oxidation method after the addition of H_2O_2. The totally golden yellow color indicated that the just mentioned modified process can be used to obtain excellent quality of GO.

The Raman spectrum reflects structural changes occurring in graphite and GO (Figure 3). Highly ordered graphite has a couple of Raman-active bands visible in the spectra, the in-phase vibration of the graphic lattice (G band at 1565 cm^{-1}), and the weak disorder band caused by the graphite edges (D band at 1343 cm^{-1}). Both the G and the D band undergo significant changes upon oxidation and exfoliation of graphite as GO contains a certain fraction of sp^3 carbons. In the case of GO, the D band shifts to 1355 cm^{-1}, and becomes broader with higher relative intensity compared with that of the G band, which indicates the higher disorder in GO. The broader G band also indicated the deconstruction of highly ordered graphite. Moreover, the blue shift of G band to 1595 cm^{-1} is mainly due to the isolated double bonds of GO resonate at higher frequencies than that in graphite.[25]

AFM was performed to observe the morphology of GO. It can be seen from the AFM profile that GO is fairly small (around 1 μm) and ultrathin. The thickness of GO is 0.8 to 1.2 nm (see Figure 4) which is typical for a one-atom-thick GO nanolayer. Such a small thickness indicates that the specific surface area of GO must be very large, which is important for polymer/layered compound nanocomposites.[26] The layers are a bit thicker than individual graphene due to the presence of oxygenated functional groups such as hydroxyl, carboxyl, and epoxy, which disrupt the original conjugation and introduce lattice defects to form folds and distortions on the GO layers. Such disruption and lattice defects reduce the mechanical strength of the GO layers.

The XPS measurement was carried out to further investigate the surface structure of GO. The C/O atomic ratio (64/36%) of GO confirms the success of graphite oxidation [see Figure 5(a)]. The C1s XPS spectra of GO [Figure 5(b)] present three types of carbon: the nonoxygenated ring carbon C–C (284.5 eV), C–O (286.5 eV), and O–C=O (289.0 eV), in a good agreement with earlier work.[27] The peak for O–C=O is very weak, indicating infrequent carboxyl group attached to the GO.

Mechanical Properties of PU/GO Nanocomposites

The typical tensile stress-strain curves for neat PU and PU/GO nanocomposites are shown in Supporting Information Figure S1. Table I summarizes the tensile mechanical properties of neat PU and PU/GO nanocomposites. In Table I, one can see that the elongation at break and toughness of neat PU were effectively improved by the addition of GO. These expected improvements in the elongation at break and toughness of PU matrix attributed to the chemical interaction between GO and PU matrix. The oxygen-containing functional groups such as hydroxyl groups on GO can react easily with diisocyanate groups of IPDI; however, it is not easy to get any evidence of improved chemical or physical interactions in the Fourier Transform-Infrared Spectrometer spectra because of the low concentration of GO in this study. It has been proved in literature that the variety of the mechanical properties of TPU/GO composites is due to the effects of GO on the crystallinity of both soft and hard segments.[18] However, the bio-based PU matrix employed in this study is an amorphous thermosetting resin. The effect of GO on the mechanical properties of thermosetting PU matrix is different from that of thermoplastic PU. As for the thermosetting bio-based PU matrix, polyol is the primary soft segment while GO can be considered as a secondary soft segment, where the GO can be viewed as two-dimensional random diblock soft segment with one graphitic block and another highly oxidized block.[28] For the current study, toughness of PU increased while strength and modulus decreased by incorporating GO due to the formation of new secondary soft segment. However, it has been reported in literature that the elongation at break and toughness decreased while strength and modulus increased for TPU/GO nanocomposites due to the diversification of the crystallinity of both soft and hard segments.[18]

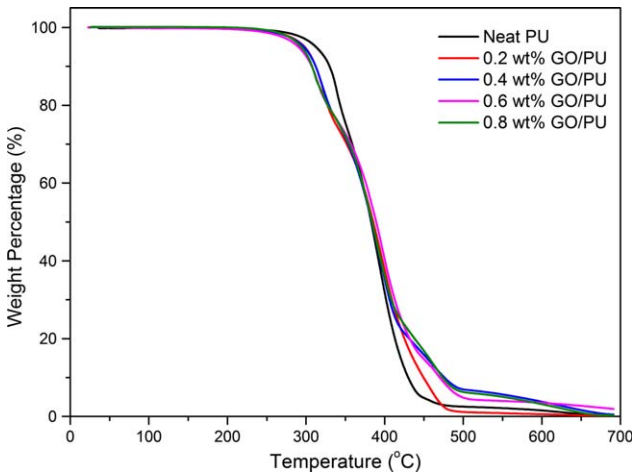

Figure 6. TGA measurement for PU/GO nanocomposites at 20°C/min heating rate under a nitrogen atmosphere. [Color figure can be viewed in the online issue, which is available at wileyonlinelibrary.com.]

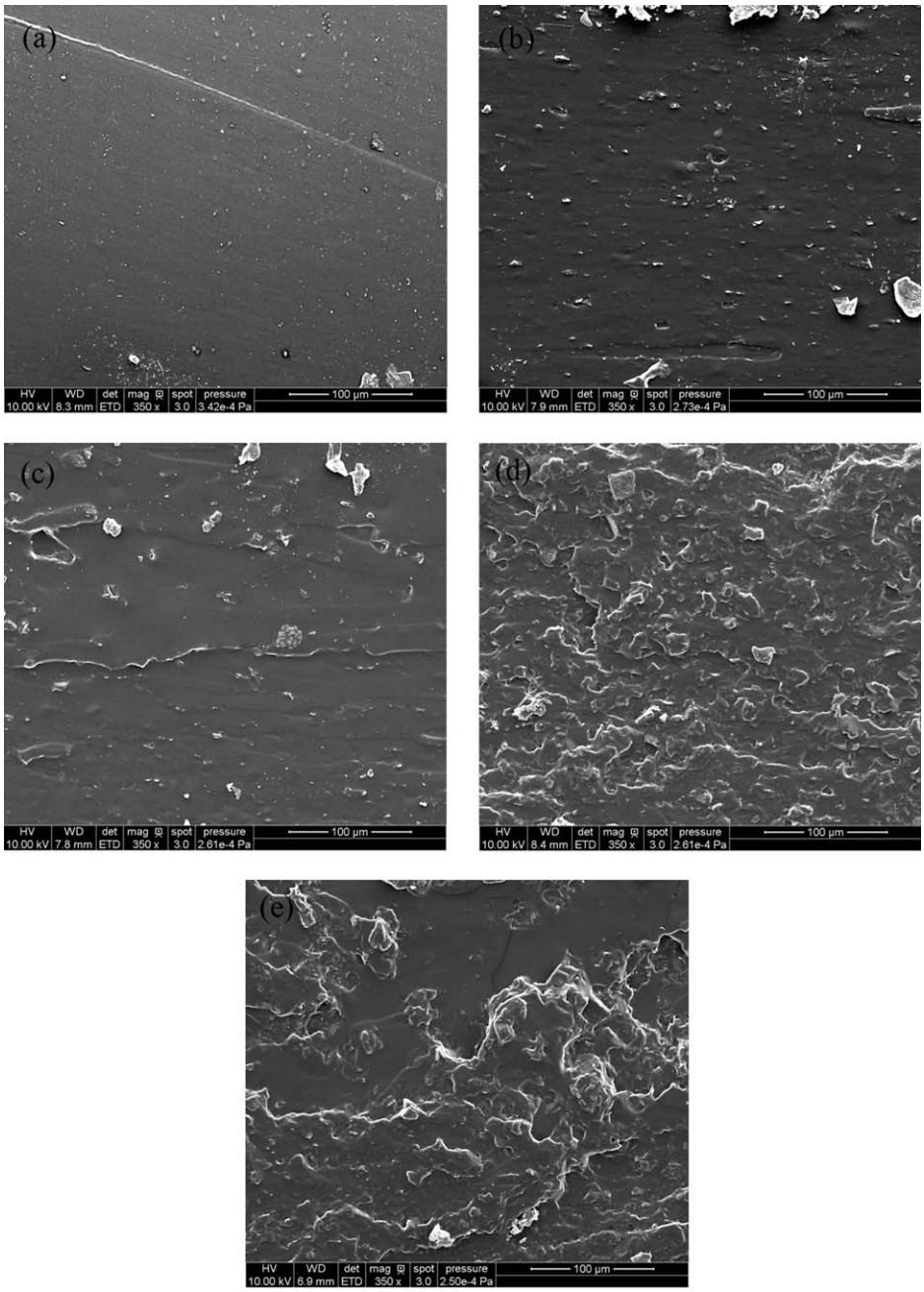

Figure 7. SEM images of (a) neat PU, (b) 0.2 wt % GO nanocomposite, (c) 0.4 wt % GO nanocomposite, (d) 0.6 wt % GO nanocomposite, and (e) 0.8 wt % GO nanocomposite.

Thermomechanical Properties of PU/GO Nanocomposites

The DMA measurements for pure bio-based PU and PU/GO nancomposites for different GO contents are shown in Supporting Information Figure S2(a) which demonstrates temperature dependence of storage modulus for different GO contents. Table II summarizes the thermal properties of neat PU and PU/GO nanocomposites. Clearly, storage modulus increases systematically with increasing the content of GO up to 0.4 wt %. For example in the glassy state, at −80°C, the storage modulus increases from 1335 MPa for neat PU to approximately 1615 MPa (21% increase) with 0.4% GO. However, it decreases with higher GO contents. This can be ascribed to the excessive GO which hinders the cross-linking between the polyol soft segment and the IPDI hard segment. Higher concentration of GO might have a negative impact on the reaction of polyols with diiscoyante and consequently reduce the cross-linking density and decrease the mechanical properties. As showed in Table I, both the elongation at break and the toughness of PU/GO nanocomposites also increased until 0.4 wt % GO, then decreased with more contents of GO. As the temperature increases, the storage modulus falls, indicating energy dissipation which occurs during the transition of the glassy state to a rubber state. For neat PU,

the energy dissipation begins at about 6°C which can be seen from the loss tangent curves [see Supporting Information Figure S2(b)]. Due to the introduction of new secondary GO soft segment, the initial transition temperatures of nanocomposites containing small amounts of GO (less than 0.4%) shift to lower temperatures of about −12°C, and their relaxation occurs in a wider temperature range. With higher contents of GO filler (more than 0.4%), the initial transition temperatures of the nanocomposites increase compared with that of the low GO content nanocomposites. It is due to the lamellar barrier effect of the excessive GO restricting the segmental motion of the polymer chains in the matrix at the glassy state. The glass transition temperature (T_g) is named as the loss factor (tan delta) peaks to maximum. Around T_g, the response of segments to the imposed load becomes significant. The T_g occurs at 35.9°C for neat PU, whereas it shifts to lower temperatures for nanocomposites, presumably due to the new secondary soft segment and cross-linking density reduction. It could be inferred that the GO highly influences the molecular dynamics and cross-linking density of the thermosetting PU matrix, thereby increasing the storage modulus and reducing the T_g of the nanocomposites.

The DSC temperature scans for PU/GO nanocomposites with different GO contents are shown in Supporting Information Figure S3, and the obtained data are provided in Table II. The difference between the T_g values obtained from DSC and DMA tests is due to the different principles of the two methods. DSC measures the change in heat capacity from frozen to unfrozen chains, while DMA measures the change in the mechanical response of the polymer chains. For DSC test, T_g of the samples were determined from the midpoint temperature in the heat capacity change of nonisothermal scan. The values of the T_gs obtained by DSC are much lower than that obtained by DMA. This is a very common behavior because the alpha-relaxation process observed in the DMA measurement is frequency dependent and normally appears above the calorimetric T_g of the material. The heat capacity change step became obscure with the increasing amount of GO, which indicated that the GO/PU composites relax in a wider temperature range compared with neat PU. The data from DSC also prove that the GO act as secondary soft segment in the bio-based thermosetting PU matrix other than stiff nanofiller.

The thermal stability of the PU/GO nanocomposites was investigated using TGA. Figure 6 demonstrates a typical TGA measurement for PU/GO nanocomposites at 20°C/min heating rate under a nitrogen atmosphere. Clearly all samples are thermally stable at temperatures up to 290°C. The onset of the thermal degradation process of all PU/GO nanocomposites is almost identical and slightly lower than that of pure PU. It is also clear from this figure that the soft segments of PU start to degrade first at 290 to 370°C and the hard segments degrades later on at a temperature higher than 370°C. The nancomposites have more thermal stability at temperature higher than 400°C. In addition the PU/GO nanocomposites with GO ≥0.4 wt % have about 5 wt % inert residues, while the pure PU and PU/GO with 0.2 wt % GO have no any inert residue remaining. In conclusion incorporation of GO does not significantly enhance the thermal stability of PU under a nitrogen atmosphere.

Morphology of PU/GO Nanocomposites

It is well-known that the properties of polymer nanocomposites are strongly influenced by both the dispersion and interface interaction of nanoscale reinforcements. In order to get more information of the interface interaction between GO reinforcement and PU matrix, and the dispersion of GO nanosheets, the fracture surface of the PU/GO nanocomposites with different GO contents were investigated by SEM. As shown in Figure 7 the fracture surface of the neat PU film after tensile testing is relatively smooth, and exhibit stiffness. While the fracture surfaces of the PU/GO films after tensile testing become rough, and exhibit toughness until the concentration of GO reaches 0.4%. Moreover, most GO nanosheets were well dispersed and embedded into the PU matrix with the concentration of GO no more than 0.4%. With the addition of more GO, it began to aggregate, and the fracture-surface images of the films exhibit a stack of sheets (bright stripe), just like that of the GO membranes, which provided a barrier to cure by physically blocking functional group diffusion. The evolution of the morphology of PU/GO nanocomposites is consistent with the result from DMA investigation.

CONCLUSIONS

Surface modified nanostructured GO was successfully prepared via a modified pressurized oxidation method through the diffusion of GO into $KMnO_4/H_2SO_4$ solution under high pressure to enhance the interaction with polyurethane matrix. Incorporation of small amount of surface modified GO was found to have a considerable improvement in the mechanical and thermal properties of PU/GO nanocomposites. The elongation at break of the PU was improved by 1.3 times, and the toughness was improved by 0.8 times with the incorporation of 0.4 wt % GO, while the strength and modulus of the PU slightly decreased upon the introduction of GO. These expected improvements in the elongation at break and toughness of PU matrix attributed to the chemical interaction between GO and PU matrix. The oxygen-containing functional groups such as hydroxyl groups on GO can react easily with diisocyanate groups of IPDI during the *in situ* polymerization of PU/GO nanocomposites. The DMA revealed that, storage modulus of the PU increased systematically with increasing the content of GO up to 0.4 wt % and decreased with higher concentration of GO. This can be ascribed to the excessive GO which hinders the cross-linking between the polyols soft segments and the IPDI hard segments. Based on this experimental fact, it is apparent that the higher concentration of GO might have a negative impact on the reaction of polyols with diiscoyante and consequently reduce the cross-linking density. The T_g determined by DSC and DMA were strongly influenced by the GO content, i.e., the T_g of PU shifts to lower temperatures by adding GO due to the considerable reduction in the cross-linking density. In addition, incorporation of GO does not significantly enhance the thermal stability of PU under a nitrogen atmosphere.

ACKNOWLEDGMENTS

This work was supported by the Jiangsu Government Scholarship for Overseas Studies. The authors are also thankful to Rui Ding

and Ruqi Chen from the Department of Materials Science and Technology at Iowa State University (ISU) for the XPS characterization.

REFERENCES

1. Delebecq, E.; Pascault, J. P.; Boutevin, B.; Ganachaud, F. *Chem. Rev.* **2013**, *113*, 80.
2. Wei, X.; Yu, X. H. *J. Polym. Sci. Part B: Polym. Phys.* **1997**, *35*, 225.
3. Wei, X.; He, Q.; Yu, X. H. *J. Appl. Polym. Sci.* **1998**, *67*, 2179.
4. Petrovic, Z. S.; Ferguson, J. *Prog. Polym. Sci.* **1991**, *16*, 695.
5. Miller, J. A.; Hwang, K. K. S.; Cooper, S. L. *J. Macromol. Sci. Phys.* **1983**, *B22*, 321.
6. Visser, S. A.; Cooper, S. L. *Macromolecules* **1991**, *24*, 2584.
7. Campanella, A.; Bonnaillie, L. M.; Wool, R. P. *J. Appl. Polym. Sci.* **2009**, *112*, 2567.
8. Kong, X.; Narine, S. S. *Biomacromolecules* **2007**, *8*, 2203.
9. Kong, X. H.; Yue, J.; Narine, S. S. *Biomacromolecules* **2007**, *8*, 3584.
10. Chian, K. S.; Gan, L. H. *J. Appl. Polym. Sci.* **1998**, *68*, 509.
11. Tanaka, R.; Hirose, S.; Hatakeyama, H. *Bioresour. Technol.* **2008**, *99*, 3810.
12. Zlatanic, A.; Lava, C.; Zhang, W.; Petrovic, Z. S. *J. Polym. Sci. Part B: Polym. Phys.* **2004**, *42*, 809.
13. Sharma, V.; Banait, J. S.; Kundu, P. P. *J. Appl. Polym. Sci.* **2009**, *114*, 446.
14. de Souza, V. H. R.; Silva, S. A.; Ramos, L. P.; Zawadzki, S. F. *J. Am. Oil Chem. Soc.* **2012**, *89*, 1723.
15. Nguyen, D. A.; Lee, Y. R.; Raghu, A. V.; Jeong, H. M.; Shin, C. M.; Kim, B. K. *Polym. Int.* **2009**, *58*, 412.
16. Cai, D. Y.; Jin, J.; Yusoh, K.; Rafiq, R.; Song, M. *Compos. Sci. Technol.* **2012**, *72*, 702.
17. Kim, H.; Miura, Y.; Macosko, C. W. *Chem. Mater.* **2010**, *22*, 344.
18. Lee, Y. R.; Raghu, A. V.; Jeong, H. M.; Kim, B. K. *Macromol. Chem. Phys.* **2009**, *210*, 1247.
19. Wang, X.; Hu, Y. A.; Song, L.; Yang, H. Y.; Xing, W. Y.; Lu, H. D. *J. Mater. Chem.* **2011**, *21*, 4222.
20. Chen, Z. X.; Lu, H. B. *J. Mater. Chem.* **2012**, *22*, 12479.
21. Zhang, C. Q.; Xia, Y.; Chen, R. Q.; Huh, S.; Johnston, P. A.; Kessler, M. R. *Green Chem.* **2013**, *15*, 1477.
22. Hummers, W. S.; Offeman, R. E. *J. Am. Chem. Soc.* **1958**, *80*, 1339.
23. Staudenmaier, L. *Ber. Dtsch. Chem. Ges.* **1898**, *32*, 1394.
24. Bao, C. L.; Song, L.; Xing, W. Y.; Yuan, B. H.; Wilkie, C. A.; Huang, J. L.; Guo, Y. Q.; Hu, Y. *J. Mater. Chem.* **2012**, *22*, 6088.
25. Kudin, K. N.; Ozbas, B.; Schniepp, H. C.; Prud'homme, R. K.; Aksay, L. A.; Car, R. *Nano Lett.* **2008**, *8*, 36.
26. Khan, U.; May, P.; O'Neill, A.; Coleman, J. N. *Carbon* **2010**, *48*, 4035.
27. Paredes, J. I.; Villar-Rodil, S.; Martinez-Alonso, A.; Tascon, J. M. D. *Langmuir* **2008**, *24*, 10560.
28. Kim, J.; Cote, L. J.; Huang, J. X. *Accounts Chem. Res.* **2012**, *45*, 1356.